Int. J. Electrochem. Sci., 13 **(2018)** 11777 – 11786, doi: 10.20964/2018.12.77

International Journal of
ELECTROCHEMICAL
SCIENCE
www.electrochemsci.org

Short Communication

Design, Fabrication and Investigation of Semitransparent Thermoelectric Cells Based on Graphene

Muhammad Tariq Saeed Chani[1*], *Khasan S. Karimov*[2,3], *Jameel-un Nabi*[2], *Muhammad Hashim*[2] , *Iqra Kiran*[2], *Abdullah M Asiri*[1,4]

[1]Chemistry Department, Faculty of Science, King Abdulaziz University, Jeddah 21589, P.O. Box 80203, Saudi Arabia
[2] Ghulam Ishaq Khan Institute of Engineering Sciences and Technology, Topi-23640, District Swabi, KPK, Pakistan
[3]Center for Innovative Development of Science and New Technologies of Academy of Sciences of Tajikistan, Dushanbe, 734025, Rudaki 33, Tajikistan
[4]Center of Excellence for Advanced Materials Research, King Abdulaziz University, Jeddah 21589,P.O. Box 80203, Saudi Arabia
[*]E-mail: tariqchani1@gmail.com, ceamr3@gmail.com

Received: 5 September 2018/ *Accepted:* 12 October 2018 / *Published:* 5 November 2018

The design, fabrication and investigation of the graphene-In-SnO_2 (indium tin oxide (ITO)) based bi-layer semitransparent thermoelectric cells are described. The cells were fabricated by encapsulating the graphene powder in the form of narrow strips on the transparent flexible plastic substrates covered by ITO. Between the parallel graphene strips, there were transparent ITO strips of the same width. This structure made the thermoelectric cells semitransparent. It was observed that Seebeck coefficient and figure of merit of the thermoelectric cell increased with temperature. The output voltage of the cells also increased with increase in gradient of temperature. The obtained results may be used for the development of the semitransparent solar thermoelectric cells because this technology is cheaper and simple as compared to semitransparent solar cells technologies.

Keywords: Encapsulation, Seebeck coefficient; temperature gradient; flexible substrate; figure of merit.

1. INTRODUCTION

A significant interest has been developed in room temperature thermoelectric energy recovery due to the application of various heat sources close to the room temperature. These sources include solar cells, consumer electronics, human body's wearable devices and home heating. Recently, various non-transparent materials with fascinating thermoelectric properties were reported for application in

renewable power-generation. These materials include silicides, half-Heuslers and tellurides [1-4]. Currently, very few transparent (optically) devices exist but the realization of these transparent devices will cause to open new fields in various novel applications like smart screens/windows and fast power recovery and on-chip cooling.

During the last few years numerous semitransparent solar cells were designed, fabricated and experimentally tested [5-9]. The semitransparent organic solar cells were fabricated on the base of polymer/fullerene blend and the sputtered aluminium doped zinc oxide cathodes. These cathodes had a pleasant color, while the cells had a power conversion efficiency $\eta \approx 3$ % [10]. An ITO-free silver nanowire electrode based semitransparent organic solar-cells (OSCs) having high fill factor were fabricated fully by the solution process method [6]. By using silver nanowires as bottom and top electrodes a high fill factor (up to 63.0) was obtained which was comparable to that of ITO based devices. These results indicate that the fully printed, fully solution processed semi-transparent and non-transparent ITO free OSCs may be comprehended without any loss.

The outputs of the semitransparent solar cells are the electric power and the light; a part of incident light coverts in to electric power, while the other part penetrates through the cell [8]. These cells can be applied in the walls, roofs and the windows of the buildings. The solar cells based on chalcopyrite, amorphous silicon, kesterite, perovskite, CdTe, dye-sensitized and organic materials can be employed for these applications. The higher efficiency gains can be obtained by these technologies. It was described that the transparency of the perovskite solar cell can be enhanced by reducing the optical-scattering at perovskite layer by ultra-smoothing of its surface [7]. In this study the short spinning method along with vacuum drying was used to deposit ultra-smooth (roughness: 6nm) perovskite films and the prepared cell had a power conversion efficiency of 14.26 %.

A colloidal quantum dots based transparent, highly efficient and stable solar cell was fabricated, which had 20.4 % average transmittance and 7.3 % efficiency [9]. The planar perovskite based inverted semitransparent solar cells with 16.1 % efficiency were fabricated that showed up to -0.18 % $^{\circ}C^{-1}$ temperature coefficient. These devices showed 80.4 % transmittance in the range of 800 to 1200 nm, which leads to thin films tandem devices having 20.9 % and 22.1 % efficiency for $CuInSe_2$ and $Cu(In, Ga)Se_2$ bottom cells, correspondingly [10]. The study of the opto-electrical effect on the perovskite based semitransparent solar cells connected with mirrors (dielectric) described that a 21 % enhancement in photocurrent density was observed in a cell with 4.2 % efficiency and 31 % transparency [11]. The indium-free semitransparent flexible perovskite solar cells with ultrathin metallic electrodes were fabricated and their visible transparency and power conversion efficiency were 18.16 % and 6.96 %, respectively, in the wavelength range of 390 to 780 nm [12]. The investigation of CIGS ($Cu(In, Ga)Se_2$) cell showed that in term of conversion efficiency and stability this is more advantageous cell as compared to all thin-film-based solar cells [13]. The semitransparent solar cells with ITO and ITO-free (ITO replaced by MoO_3-Ag-TiO_2 (MAT)) were investigated and it was found that the MAT cell was cheaper than the ITO based cell, but less stable [14].

The investigation of semitransparent solar cell's structure, properties and characteristic shows that the semitransparent cells are less efficient as compared to opaque cells and their fabrication is complex because of thin films deposition. So, the thermoelectric-cells and generators (TEGs) are the alternative approach, which are simple in structure due to lack of Schottky or p-n junctions and

multilayers [15, 16]. As for as efficiency is concerned, recently a *p*-type compound (MgAgSb) based thermoelectric-leg showed 8.5 % efficiency in 20 to 245 °C temperature range [17]. By raising hot side's temperature up to 295 °C the 10% increase in efficiency may achieved that is comparable to solar cell efficiency. To eliminate the conventional metallization process the one-step hot-press technique was used for silver contact pads deposition. By this the simplified manufacturing of the thermoelectric elements with low contact resistances (thermal and electrical) becomes viable.

For the determination of thermoelectric cell efficiency (Z) the following relationship was derived by Ioffe [18]:

$$Z = \frac{\sigma\alpha^2}{k} \quad (1)$$

where, σ is the electrical conductivity and k is thermal conductivity, while the α is Seebeck coefficient. The *ZT*, a dimensionless-figure of merit was presented latterly as well [19]. The *ZT* is a product of average temperature (*T*) and *Z*.

$$\bar{T} = \frac{T_1+T_2}{2} \quad (2)$$

where, T_1 and T_2 are temperatures of two contacts.

Depending upon some conditions, the higher *ZT* causes higher efficiency especially when the two materials of the couple have similar *Z* values. The *ZT* is thought to be a method by which the potential thermoelectric efficiencies of the devices can be compared using various materials. The 1 is thought good value for *ZT*; but for the efficiency competition with mechanical devices the *ZT* values from 3 to 4 are important. So far, the *ZT* highest reported value is ~ 2 [20, 21]. The reduction in *k* and the increase in α through nanostructure manipulation is the prime focus of the thermoelectric material's research.

The following expression is used to determine the Maximum energy efficiency:

$$\eta_{max} = \frac{T_H - T_C}{T_H} \frac{\sqrt{1+Z\bar{T}} - 1}{\sqrt{1+Z\bar{T}} + \frac{T_C}{T_H}}, \quad (3)$$

where, T_H and T_C are the temperature at hot junction and cold surface, correspondingly, while the $Z\bar{T}$ is modified dimension-less figure of merit, which reflects thermoelectric-capacity of the device's materials (both materials). The $Z\bar{T}$ is presented as:

$$Z\bar{T} = \frac{(\alpha_p-\alpha_n)^2\bar{T}}{[(\rho_n k_n)^{1/2} + (\rho_p k_p)^{1/2}]^2} \quad (4)$$

where, ρ and $\bar{T}$ are the electrical resistivity and the average temperature (b/w cold and hot surfaces), respectively. The *p* and n subscripts specifying the characteristics related to semiconducting *p* and *n* type thermoelectric materials, correspondingly.

The thermoelectric properties of the graphene were investigated in a number of papers: an enormous thermoelectric effect was observed in graphene [22], the enhancement of the thermoelectric figure of merit by disorder in armchair graphene-nanoribbons was investigated in ref. [23], the enhancement of figure of merit (thermoelectric) in the edge-disordered zigzag graphene-nanoribbons was found in ref. [24], thermopower enhancement of graphene films by oxygen-plasma treatment was registered in [25].

For the energy conversion by using thermoelectric cells, the graphene has two disadvantages [26]. First of all: the graphene has no gap in the energy band diagram that results in a small Seebeck coefficient because of opposite contributions of holes and electrons. Secondly, the thermal conduction of the grapheme is large, which results in small ZT (thermoelectric figure of merit) of 2D (two dimensional) graphene sheets. At the same time the band gap engineering and nano-structuring of the graphene may decrease the lattice thermal-conductance and increase the Seebeck coefficient. Therefore, the graphene may be potentially used for the energy conversion [26].

The nano-structuring is one of the promising ways for the designing of thermoelectric materials. It was demonstrated theoretically that the graphene nano-ribbons with nano-pores and heavy atoms would be useful for the thermoelectric applications [27]. Through bulk the lattice thermal conduction is obstructed by a two-dimensional array of nano-pores. At T≃40 K the thermoelectric figure of merit approached to its maximum $ZT \simeq 3$.

The spin valve based on the zigzag graphene nano-ribbon (ZGNR) electrodes having various magnetic configurations was investigated for the spin-dependency of the thermoelectric effects by applying first principles calculations along with non-equilibrium Green's function [28]. It was found that the ZGNR based spin valve's electron transport properties are highly dependent on the magnetic configurations. Without considering phonon-scattering the ZT value at room temperature may reach up to 0.15.

The electronic transport and electronic states properties of graphene (graphite single sheet) and CNTs (cylindrical graphite sheet) were discussed in a review [29]. The electronic motion in the graphene was considered like a neutrino or vanishing mass Dirac electron (relativistic). The energy bands in the carbon nanotubes were determined. It was found that on flux vanishing the nanotube becomes metallic, while the flux is non-zero semiconducting. It was suggested that instead of zero-gap semiconductor the graphene should be considered as a metal. At the same time various schemes were proposed and tested about the band gap opening in graphene [29].

In continuation of our work on renewable energy devices [30-35] and by keeping in view the potential advantages of the semitransparent power generating devices (i.e. solar cells), to the best of our knowledge, we are presenting first time the design, fabrication, investigation and properties of the semitransparent thermoelectric cells based on graphene and ITO bi-layer cells.

2. EXPERIMENTAL

The In-SnO_2 (indium tin oxide (ITO)) coated flexible substrates and the graphene were purchased from Sigma Aldrich. Figure 1 shows the schematic diagrams of the two-dimensional graphene structure [36]. For the fabrication of semitransparent thermoelectric cells the flexible transparent substrates of sizes of 25 mm x 25 mm x 1 mm covered with ITO were used. Figure 2 (a) shows the top and the front views of the schematic diagram of the fabricated thermoelectric cells. The length, width and the thickness of the graphene strips were equal to 15 x 5 x 0.28 mm^3. The distance between the strips was equal to 4-6 mm. The gradient of temperature (8 $^{\circ}$C) was created in the samples along the graphene strips (Fig.2) by using the electric heaters.

The structures of the fabricated thermoelectric cells is shown in Fig. 2 (b). The difference of temperatures in the substrates along the graphene strips was measured by FLUKE 87 multimeter. The voltages generated due to the thermoelectric effect in the cells were measured by HIOKI DT 4252 digital multimeter. The transparency of the samples was in the range of 50-55 %.

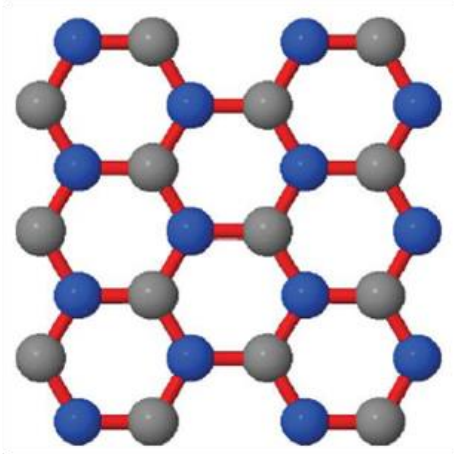

Figure 1. The schematic diagram of a two-dimensional graphene layer [36].

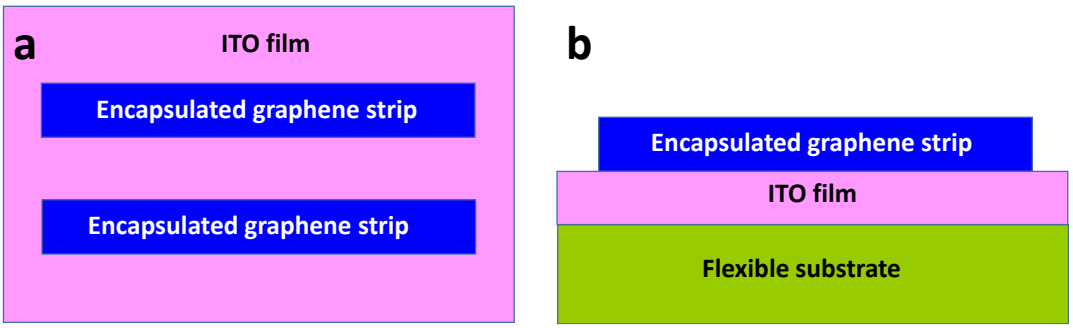

Figure 2. Schematic top view (a) and front view (b) of the bi-layer thermoelectric cells.

3. RESULTS AND DISCUSSION

First of all the thermoelectric properties of the only ITO (In-SnO_2) samples before encapsulation of the graphene strips were investigated. It was found that the thermoelectric coefficient was equal to -22.5 µV/K for ITO covered flexible plastic substrate. In ref. [37] it was shown that ITO thin films are *n*-type semiconductor, with the wide energy gap of 3.6-3.8, eV, and with optical transparency. If the ITO is doped by Fe or Cu then it shows *p*-type conduction [37].

Figure 3 shows the dependence of the Seebeck coefficient of the graphene-ITO based cell on temperature. It can be seen that in the temperature range of 302-313 K the Seebeck coefficient increases from 25 µV/K to 35 µV/K. This value is higher than the already reported value for single-layer graphene (23 µV/K) [25, 38].

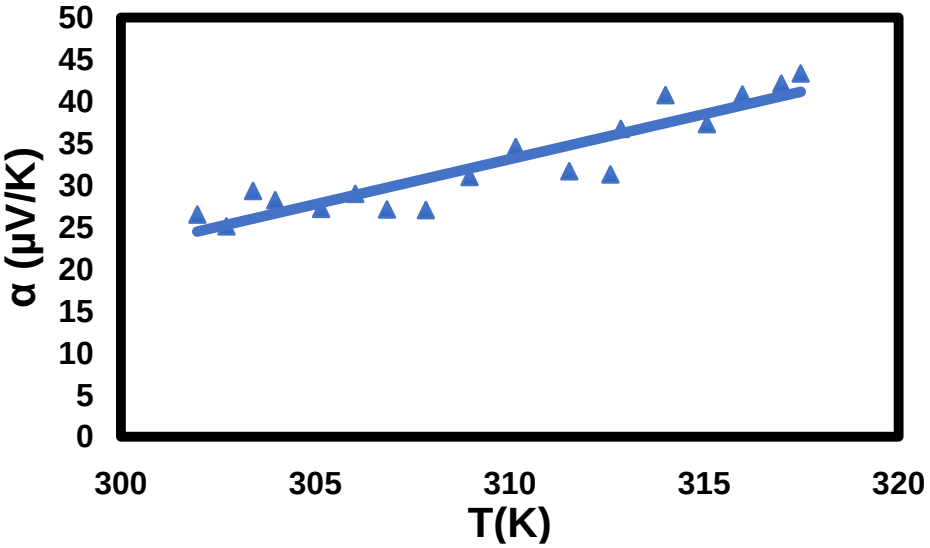

Figure 3. Dependence of Seebeck coefficient on temperature for the graphene-ITO based cell.

The Fig.3 shows that the Seebeck coefficient increases with increase in temperature. This behavior is similar to that which was observed for metals [36, 39]. Figure 4 shows the dependence of the output voltage of the thermoelectric cell on the gradient of temperature. It shows a linear behavior.

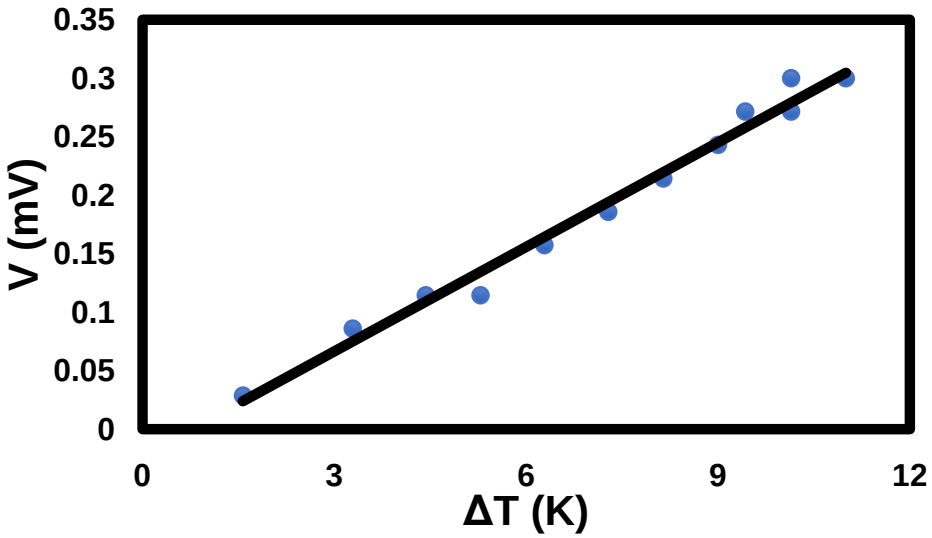

Figure 4. Dependence of the output voltage on the temperature gradient for the graphene-ITO based cell.

By using the values of electrical conductivity of graphene (10^4 S/m at T=300 K) and its thermal conductivity (175 kW/mk at a temperature of 300 K [40], the figure of merit (*ZT*) can be calculated. The Fig.5 shows the dependence of the figure of merit (*ZT*) on the temperature for the investigated graphene-ITO cell. It can be seen that *ZT* increases with increase in temperature. Figure 6 shows the dependence of the efficiency (*Ƞ*) of the graphene-ITO cell on the temperature. It can be seen that the efficiency increases with increase in temperature.

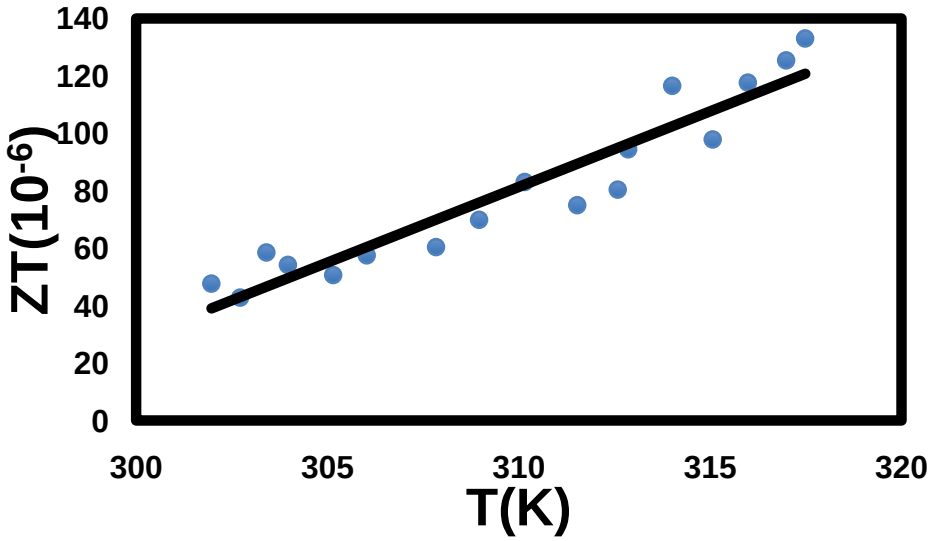

Figure 5. Dependence of the figure of merit (*ZT*) on the temperature for the investigated graphene-ITO semitransparent thermoelectric cell.

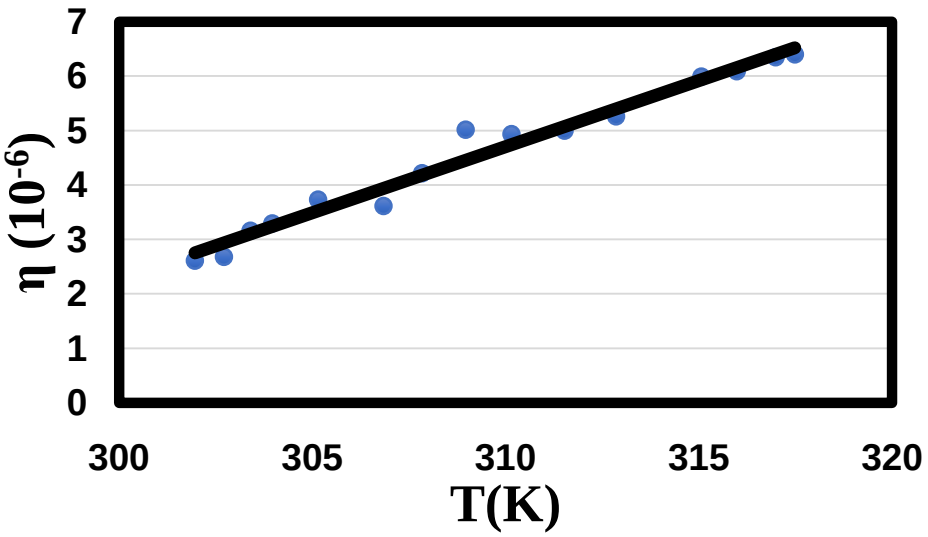

Figure 6. Dependence of the efficiency (Ƞ) of the graphene-ITO thermoelectric sample on the temperature.

The Seebeck coefficient usually increases with temperature in a number of metals [41]. On the contrary in general the thermoelectric coefficient decreases with increase in temperature in semiconductors, but the actual behavior depends upon the type of semiconductor, impurities that are available and their concentrations [41].

The Seebeck coefficient for the metals is determined by the following expression [39]:

$\alpha \approx C_{el}/q \approx (k_B/e)(k_BT/E_F)$ (5)

Accordingly for the semiconductors:

$\alpha \approx C_{el}/q \approx (k_B/e)(E_g/k_BT)$ (6)

The experimental results shown in Fig.3 formally follow the Eq.5. In reality the investigated semitransparent thermoelectric cells are not simple but compound, or bi-layer structure (ITO + graphene). The thermopower (α) for different types of carrier is given by a weighted average of their electrical conductivity values (σ_n and σ_p) [39]:

$$\alpha \approx(\alpha_n\sigma_n + \alpha_p\sigma_p) / (\sigma_n + \sigma_p) \quad (7)$$

This case with some approximation can be used for the understanding of the thermoelectric behavior of the bi-layer ITO-graphene system.

These results can be used for further development of the semitransparent thermoelectric cells, in particular for the semitransparent solar energy conversion thermoelectric cells. Our preliminary investigation showed that the plane cells can be used as a prototype for the development of semitransparent solar thermoelectric cells: the flexible plastic transparent conductive substrates covered by ITO have three basic parts: plane semitransparent part which covers 50-70% of the area, and plane reflector and plane collector which are placed in opposite position from two sides of the semitransparent part.

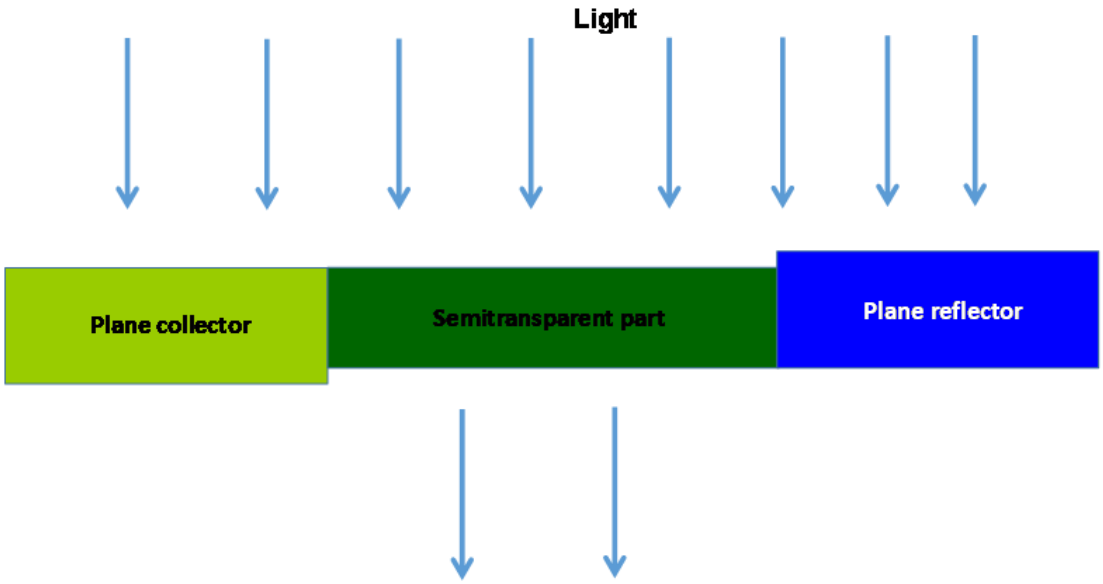

Figure 7. Simplified prototype of the semitransparent solar thermoelectric cell.

As the reflector reflects light and the collector absorbs the light resultantly a gradient of temperature is developed which generates the voltage. In these plastic substrate based simplified plane cells the gradient of 4 to 5 °C was obtained practically under the illumination of 140 W/m^2 (generated by filament lamp). The optimization of the shape of the semitransparent thermoelectric cell definitely allows the increasing of the temperature gradient at the same illumination that would be matter of our future research.

4. CONCLUSION

This work presents the design, fabrication and investigation of the properties of the flexible bilayer semitransparent thermoelectric cells based on graphene and ITO. It was found that the fabricated cells can be used potentially for the demonstrative purposes for the development of semitransparent thermoelectric cells which can produce electric power and provide illumination in the environment. It was observed in the bi-layer graphene-ITO cells that the thermoelectric properties (i.e. Seebeck coefficient) of the graphene (by sign and value) are dominating over the ITO, which gives positive sign to the Seebeck coefficient of the bi-layer cells. Due to ease in fabrication these thermoelectric cells may be used as teaching aid. Replacement of the graphene with other materials having higher figure of merit (ZT) will allow to increase output power and widen the scale and range of the application of the cells. To the best of our knowledge, it is the first attempt towards the realization of the semitransparent thermoelectric cells based on graphene, in particular, bi-layer grapheme-ITO structure.

ACKNOWLEDGEMENTS
This project was funded by the Deanship of Scientific Research (DSR) at King Abdulaziz University, under grant no. G-353-130-38. The authors, therefore, acknowledge with thanks DSR for technical and financial support.

References

1. C. Yang, D. Souchay, M. Kneiß, M. Bogner, H.M. Wei, M. Lorenz, O. Oeckler, G. Benstetter, Y.Q. Fu, M. Grundmann, *Nat. Commun.*, 8 (2017) 16076.
2. Y. Gelbstein, *ActaMater.*, 61 (2013) 1499-1507.
3. K. Kirievsky, M. Shlimovich, D. Fuks, Y. Gelbstein, *Phys. Chem. Chem. Phys*., 16 (2014) 20023-20029.
4. Y. Gelbstein, J. Tunbridge, R. Dixon, M.J. Reece, H. Ning, R. Gilchrist, R. Summers, I. Agote, M.A. Lagos, K. Simpson, *J. Electron. Mater*., 43 (2014) 1703-1711.
5. A. Colsmann, A. Puetz, A. Bauer, J. Hanisch, E. Ahlswede, U. Lemmer, *Adv. Energy Mater.*, 1 (2011) 599-603.
6. F. Guo, X. Zhu, K. Forberich, J. Krantz, T. Stubhan, M. Salinas, M. Halik, S. Spallek, B. Butz, E. Spiecker, T. Ameri, N. Li, P. Kubis, D.M. Guldi, G.J. Matt, C.J. Brabec, *Adv. Energy Mater.*, 3 (2013) 1062-1067.
7. G.M. Kim, T. Tatsuma, *J. Phys. Chem. C*, 120 (2016) 28933-28938.
8. J. Sun, J. Jasieniak, *J. Phys. D*, 50 (2017) 093001.
9. X. Zhang, C. Hagglund, E.M.J. Johansson, *Energy Environ. Sci.*, 10 (2017) 216-224.
10. F. Fu, T. Feurer, T.P. Weiss, S. Pisoni, E. Avancini, C. Andres, S. Buecheler, A.N. Tiwari, *Nat. Energy*, 2 (2016) 16190.
11. C.O. Ramírez Quiroz, C. Bronnbauer, I. Levchuk, Y. Hou, C.J. Brabec, K. Forberich, *ACS Nano*, 10 (2016) 5104-5112.
12. X.-L. Ou, J. Feng, M. Xu, H.-B. Sun, *Opt. Lett.*, 42 (2017) 19581961.
13. M. Saifullah, S. Ahn, J. Gwak, S. Ahn, K. Kim, J. Cho, J.H. Park, Y.J. Eo, A. Cho, J.-S. Yoo, J.H. Yun, *J. Mater. Chem. A*, 4 (2016) 10542-10551.
14. E. Voroshazi, M.B. Yaala, G. Uytterhoeven, J.G. Tait, R.H.A.J.M. Andriessen, Y. Galagan, D. Cheyns, Light stability of ITO-free semi-transparent and opaque organic photovoltaic devices, in: 2015 IEEE 42nd Photovoltaic Specialist Conference (PVSC), 2015, pp. 1-4.

15. K.S. Karimov, Organic Solar Cells, in: D.J.N. Govil (Ed.) Energy Science and Technology, *Studium Press LLC, USA*, 2015, pp. 302-321.
16. K.S. Karimov, M. Abid, K.Y. Cheong, M.M. Bashir, Thermoelectric properties of organic and inorganic materials and cells in: K.Y. Cheong (Ed.) Two-dimensional nanostructures for energy-related applications, *Taylor & Francis Group*, Boca Raton, Landon, New York, 2016, pp. 48-98.
17. D. Kraemer, J. Sui, K. McEnaney, H. Zhao, Q. Jie, Z.F. Ren, G. Chen, *Energy Environ. Sci.*, 8 (2015) 1299-1308.
18. A.F. Ioffe, *DokladyAkad. Nauk SSSR*, 87 (1952) 369.
19. A. Bulusu, D.G. Walker, *Superlattices Microstruct.*, 44 (2008) 1-36.
20. K. Biswas, J. He, I.D. Blum, C.-I. Wu, T.P. Hogan, D.N. Seidman, V.P. Dravid, M.G. Kanatzidis, *Nat.*, 489 (2012) 414-418.
21. K.F. Hsu, S. Loo, F. Guo, W. Chen, J.S. Dyck, C. Uher, T. Hogan, E. Polychroniadis, M.G. Kanatzidis, *Cubic Sci.*, 303 (2004) 818-821.
22. D. Dragoman, M. Dragoman, *Lett.*, 91 (2007) 203116.
23. X. Ni, G. Liang, J.-S. Wang, B. Li, *Appl. Phys. Lett.*, 95 (2009) 192114.
24. H. Sevinçli, G. Cuniberti, *Phys. Rev. B*, 81 (2010) 113401.
25. N. Xiao, X. Dong, L. Song, D. Liu, Y. Tay, S. Wu, L.-J. Li, Y. Zhao, T. Yu, H. Zhang, *ACS Nano*, 5 (2011) 2749-2755.
26. P. Dollfus, V.H. Nguyen, J. Saint-Martin, *J. Phys. Condens. Matter*, 27 (2015) 133204.
27. P.-H. Chang, M.S. Bahramy, N. Nagaosa, B.K. Nikolic, *Nano Lett.*, 14 (2014) 3779-3784.
28. M. Zeng, W. Huang, G. Liang, *Nanoscale*, 5 (2013) 200-208.
29. T. Ando, *NPG Asia Mater.*, 1 (2009) 17-21.
30. H.M. Marwani, M.T.S. Chani, E.Y. Danish, Kh.S. Karimov, A. Hagfeldt, A.M. Asiri, *Int. J. Electrochem. Sci*., 12 (2017) 4096-4106.
31. M.T.S. Chani, H.M. Marwani, E.Y. Danish, Kh.S. Karimov, M. Hilal, A. Hagfeldt, A.M. Asiri, *J. Optoelectron. Adv. Mater.*, 19 (2017) 178-183.
32. M.T.S. Chani, Kh.S. Karimov, H.M. Marwani, E.Y. Danish, W. Ahmad, J.U. Nabi, M. Hilal, A. Hagfeldt, A.M. Asiri, *Int. J. Electrochem. Sci*., 12 (2017) 9250-9261.
33. M.T.S. Chani, S.B. Khan, A.M. Asiri, Kh.S. Karimov, M.A. Rub, *J. Taiwan. Inst. Chem. Eng.*, 52 (2015) 93-99.
34. M.T.S. Chani, Kh.S. Karimov, A.M. Asiri, N. Ahmed, M.M. Bashir, S.B. Khan, M.A. Rub, N. Azum, *PLoS One*, 9 (2014) e95287.
35. M.T.S. Chani, Kh.S. Karimov, S.B. Khan, A.M. Asiri, *Int. J. Electrochem. Sci*., 10 (2015) 5694-5701.

36. A. Strikwerda, Should We Model Graphene as a 2D Sheet or Thin 3D Volume? 2015, (https://www.comsol.com/blogs/should-we-model-graphene-as-a-2d-sheet-or-thin-3d-volume/).
37. M.A. Batal, G. Nashed, F.H. Jneed, *J. Assoc. Arab Uni. Basic Appl. Sci.*, 15 (2014) 15-20.
38. X. Xu, Y. Wang, K. Zhang, X. Zhao, S. Bae, M. Heinrich, C.T. Bui, R. Xie, J.T. Thong, B.H. Hong, Phonon transport in suspended single layer graphene, *arXiv preprint arXiv*:1012.2937, (2010).
39. T.M. Tritt, M.A. Subramanian, *MRS Bull.*, 31 (2006) 188-198.
40. M. Li, Y. Sun, H. Xiao, X. Hu, Y. Yue, *Nanotechnol*., 26 (2015) 105703.
41. N. Cusack, P. Kendall, The absolute scale of thermoelectric power at high temperature, *Proceedings of the physical society*, 72 (1958) 898.